Available online at www.sciencedirect.com
SCIENCE DIRECT®
ELSEVIER
Journal of Nuclear Materials 321 (2003) 1–7
journal of nuclear materials
www.elsevier.com/locate/jnucmat

# Dissolution of synthetic brannerite in acidic and alkaline fluids

Y. Zhang *, B.S. Thomas, G.R. Lumpkin, M. Blackford, Z. Zhang, M. Colella, Z. Aly

*Australian Nuclear Science and Technology Organisation, Private Mail Bag 1, Menai, NSW 2234, Australia*

Received 21 October 2002; accepted 11 March 2003

**Abstract**

The dissolution of synthetic brannerite in aqueous media at 40 and 90 °C under atmospheric redox conditions has been studied. At 40 °C, the presence of phthalate as a buffer component in the pH range of 2–6 has little effect on uranium release from brannerite. Bicarbonate increases uranium release and enhances the dissolution of brannerite. Compared to $UO_2$, brannerite is more resistant to dissolution in bicarbonate solutions. In under-saturated conditions at 90 °C, the dissolution of brannerite is incongruent (preferential release of uranium) at pH 2 and nearly congruent at pH 11. TEM examinations reveal a polymorph of $TiO_2$ (pH 2 specimen) and a fibrous Ti-rich material (pH 11 specimen) as secondary phases. XPS analyses indicate the existence of U(V) and U(VI) species on the surfaces of specimens both before and after leaching, and U(VI) was the dominant component on the specimen leached in the pH 11 solution.


## 1. Introduction

Brannerite ($UTi_2O_6$), which exists naturally in many uranium ore bodies, has attracted recent attention as a minor phase in the ceramic formulations designed to immobilise surplus plutonium [1]. It belongs to the monoclinic crystal system with space group C2/m, and both U and Ti occupy distorted octahedral coordination polyhedra [2]. The mineralogy and hydrometallurgy of brannerite in some ore deposits have been extensively studied [3–5]. Several important observations have been made from these studies: (1) brannerite is more resistant than uraninite to dissolution in sulphuric acid; (2) from the compositional and leach studies, sufficient evidence exists to support the presence of coffinite ($U[SiO_4]_{1-x}[OH]_{4x}$) as an alteration product intergrowing with brannerite and (3) leach pit formation is the initial, rate-controlling step in brannerite dissolution regardless of the leach conditions [6]. In addition, brannerite is often associated with rutile and in many cases with anatase as a natural alteration product.

Previously we have reported some experimental studies on the dissolution of synthetic and natural brannerite [7–9]. In our early work, KHphthalate was used in the buffer solutions for pH 2–6. However, it has been reported that phthalate slightly enhances the dissolution of natural minerals [10]. In addition, the effect of bicarbonate in alkaline solutions on the dissolution of brannerite should be considered. The purpose of this paper is to provide data to quantify the effects of phthalate and bicarbonate on the dissolution of synthetic brannerite under atmospheric redox conditions and further elucidate the nature of the surface alteration products by transmission electron microscopy (TEM) and XPS examination of ion-beam-thinned (IBT) specimens leached in under-saturated conditions.

## 2. Experimental

### 2.1. Sample preparation

Synthetic brannerite was prepared by the alkoxide/nitrate route [11]. Stoichiometric mixtures were dried

* Corresponding author. Tel.: +61-2 9717 9156; fax: +61-2 9543 7179.
*E-mail address:* yzx@ansto.gov.au (Y. Zhang).

0022-3115/$ - see front matter © 2003 Elsevier B.V. All rights reserved.
doi:10.1016/S0022-3115(03)00203-4

and calcined in argon at 750 °C for 1 h. The calcines were wet-milled for 2 h and then dried. About 2 wt% of Ti metal was added and samples were hot-pressed at 1260 °C for 2 h under 21 MPa in graphite dies. The sample contains mainly brannerite with minor rutile inclusions (~5% $TiO_2$ and trace amounts of reduced Ti oxide) and only a trace amount of $UO_2$ (<0.1%).

The powdered sample for the dissolution tests was prepared by crushing a monolithic sample to particle sizes between 75 and 150 μm diameter and washing with acetone to remove fines from the surfaces. The surface area was measured by the BET method as 0.08 $m^2 g^{-1}$.

The IBT TEM specimens were prepared in the conventional manner, whereby a thin wafer, ~0.5 mm thick, was sectioned from the bulk specimen using a sectioning saw. A disc (~3.0 mm in diameter) was then cored from the wafer using an ultrasonic coring drill. The disc was further processed by mechanical thinning techniques down to a thickness of ~80 μm and both sides polished to ~0.25 μm. The disc was then dimpled on one side. This process introduced a polished concave surface in the disk, ~15 μm thick at the centre, minimising the time required for ion milling, while still maintaining specimen integrity at the outer rim. The dimpled specimen was ion milled using a Gatan Precision Ion Polishing System (PIPS). The parameters set for milling were 4.5 keV $Ar^+$ ions incident on the specimen at the low incident angle of ±4.5°.

### 2.2. Electron microscopy and X-ray photoelectron spectroscopy

TEM was carried out with a JEOL 2010F equipped with a Link-ISIS Energy dispersive X-ray (EDX) system, operated at 200 kV and calibrated for quantitative thin-film analyses using an extensive set of natural and synthetic reference materials [12].

The IBT TEM specimens were also analysed by XPS both before and after leach testing. XPS measurements were performed in ultra-high vacuum with a VG ESCALAB 220i-XL system employing a monochromatic Al $K_\alpha$ (1486.7 eV) X-ray source. The X-ray gun was operated at 120 W, and the spectrometer pass energy was set at 20 eV for regional scans. The diameter of the analysis area was approximately 500 μm, much larger than the average grain size (~50 μm). The thickness of the probed surface layer was <5 nm. The IBT specimens were mounted using double-sided conductive adhesive tape under a stainless steel foil with an open aperture of ~3 mm, exposing an outer rim area to be analysed. Charge compensation was achieved by using a low energy electron flood gun. The C 1s peak from the adventitious carbon was found at its standard value (285.0 ± 0.1) eV for all three samples, therefore further corrections in binding energy were unnecessary. The surface concentration of different species was determined by integrating the peak area (after subtracting a Shirley-type background) with Scofield sensitivity factors as defined in the software package supplied by VG Scientific.

### 2.3. Effects of phthalate and bicarbonate

Batch equilibrium tests were carried out in polystyrene containers on a shaking bench (once per second) within an oven at 40 °C. A series of phthalate or bicarbonate solutions with concentrations ranging from $10^{-4}$ to $10^{-2}$ M, with constant pH (pH 4 for phthalate and pH 8 for bicarbonate) and constant ionic strength (0.01 M) were used. The solution pH was adjusted using 1 M HCl and the ionic strength was adjusted using KCl. The solution compositions are summarised in Table 1. The initial solid concentration was 0.02 g in 30 ml solution. Aliquots (2 ml) were regularly taken, run through 0.25 μm filters, and acidified with 3% by volume of analytical grade $HNO_3$. An inductively coupled plasma mass spectrometer (ICP-MS) was used to determine the concentrations of U and Ti.

### 2.4. Dissolution tests for IBT specimens

Dynamic dissolution tests for IBT specimens, described elsewhere [13], were conducted at 90 °C using pH 2 ($HNO_3$ solution) and pH 11 (KOH solution) solutions and flow rates of around 50 $ml\,d^{-1}$ in an open atmosphere. The specimen was placed between Teflon sieves, and positioned near the middle of the Teflon vessel. The leachates were collected daily in the first week and then twice per week, and were acidified with 3% by volume of analytical grade $HNO_3$. ICP-MS was used to determine

Table 1
Buffer solutions used for the effect of phthalate and bicarbonate

| Solution no. | [Phthalate] (M) |
|---|---|
| P1 | $1.09\times10^{-4}$ |
| P2 | $2.14\times10^{-4}$ |
| P5 | $4.96\times10^{-4}$ |
| P10 | $1.00\times10^{-3}$ |
| P20 | $2.06\times10^{-3}$ |
| P40 | $4.00\times10^{-3}$ |
| P60 | $6.52\times10^{-3}$ |
| P100 | $1.01\times10^{-2}$ |
| | [$KHCO_3$] (M) |
| C1 | $1.04\times10^{-4}$ |
| C2 | $2.03\times10^{-4}$ |
| C5 | $5.00\times10^{-4}$ |
| C10 | $1.01\times10^{-3}$ |
| C20 | $2.02\times10^{-3}$ |
| C40 | $4.01\times10^{-3}$ |
| C60 | $6.50\times10^{-3}$ |
| C100 | $1.00\times10^{-2}$ |

the concentrations of U and Ti in the leachates. The specimens, after 4 weeks, were gently rinsed with deionised water and dried at 90 °C for TEM and XPS examinations.

## 3. Results and discussion

### 3.1. Effect of phthalate

The initial uranium release rate (at 10 min) is weakly dependent on phthalate concentration with the reaction order of $0.19 \pm 0.08$ (Fig. 1). After 1 h, the uranium release rate appears to approach a constant value. The weak rate dependence of phthalate in the first 10 min might be related to the initial dissolution of U(VI) and U(V) species present on the brannerite surface [14], which could be controlled by phthalate. In the case of titanium there is no obvious rate dependence on phthalate concentration (Fig. 2). Generally the uranium release rate is about two or three orders of magnitude higher than that of titanium (Fig. 3), indicating incongruent dissolution of brannerite.

Over the experimental time period (20 days), uranium concentrations in solutions do not seem to reach saturation. However, titanium reaches apparent equilibrium after 7 days (Fig. 4) with the saturation concentrations dependent on phthalate concentrations (Fig. 5). Therefore the phthalate ion increases titanium solubility. However, it is unlikely that slightly increasing titanium solubility would have any significant effect on uranium release since the uranium release rate is overall 100 times higher than titanium release rate with the highest phthalate concentration.

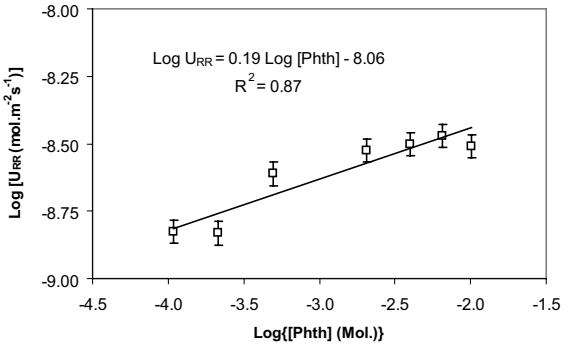


Fig. 1. The correlation between initial (10 min) uranium release rate and phthalate concentration.

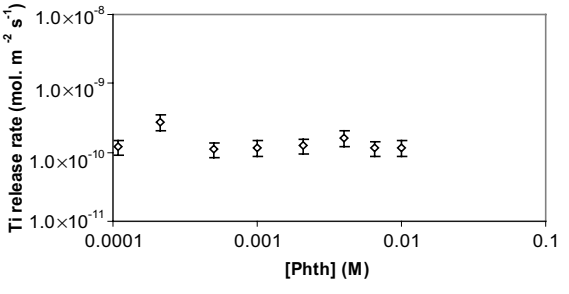


Fig. 2. The initial (10 min) titanium release rate versus phthalate concentration.

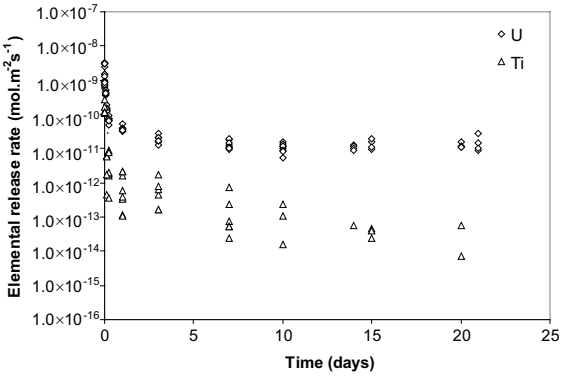


Fig. 3. Elemental release rate versus time for the tests with phthalate ($10^{-4}$–$10^{-2}$ M).

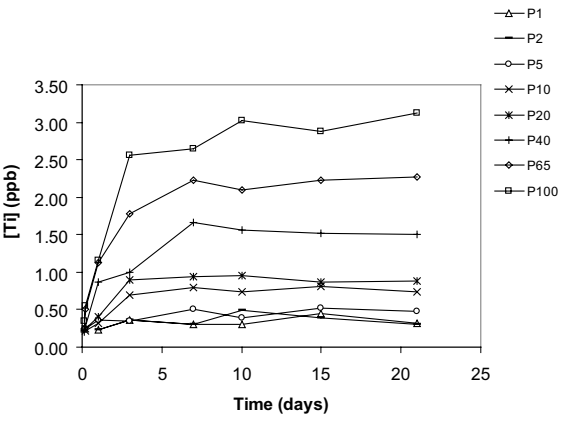


Fig. 4. Titanium concentration in phthalate solutions.

### 3.2. Effect of bicarbonate

Uranium concentrations in solutions do not reach saturation (Fig. 6) and uranium release rate is found to be dependent strongly on bicarbonate concentration over the testing time period with the reaction order varying from ~0.52 at 10 min to ~0.69 after 7 days. This implies that bicarbonate enhances the dissolution of brannerite under alkaline and atmospheric conditions. A direct comparison between brannerite (40 °C) and $UO_2$ (45 °C) [15] in bicarbonate solutions at the same

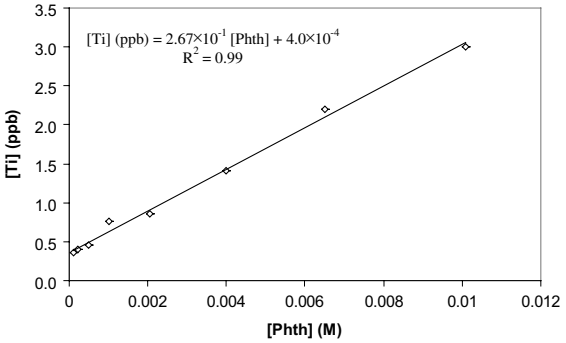


Fig. 5. Correlation between saturated Ti concentration (average values for the last three data points) and phthalate concentration.

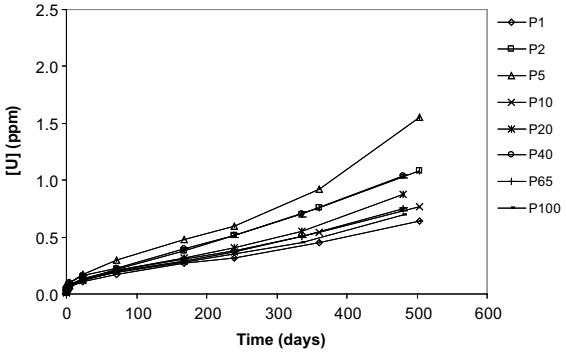


Fig. 6. Uranium concentration in bicarbonate solutions.

atmosphere and essentially the same methodology is shown in Fig. 7. The uranium release rate from brannerite is generally an order of magnitude lower than that from $UO_2$, indicating that brannerite is more resistant to dissolution than $UO_2$ in bicarbonate solutions.

Titanium releases, however, show no dependence on bicarbonate concentration at pH 8, either in release rate or equilibrium concentration (~3 ppb), indicating that unlike phthalate at pH 4, bicarbonate does not interact strongly with titanium, either on the solid surface or in solution.

### 3.3. Dissolution of IBT specimens

For pH 2 solution, the cumulative elemental releases show linear relationships versus time (Fig. 8), indicating constant (but different) release rates for both uranium and titanium. The dissolution of brannerite in pH 2 solution is incongruent and preferential release of uranium occurs (Fig. 9), as found previously [7].

In the case of pH 11 solution, the less linear and lower release of uranium than titanium (Fig. 10) suggests that some dissolved uranium may adsorb back onto the secondary phase and the sample itself or even

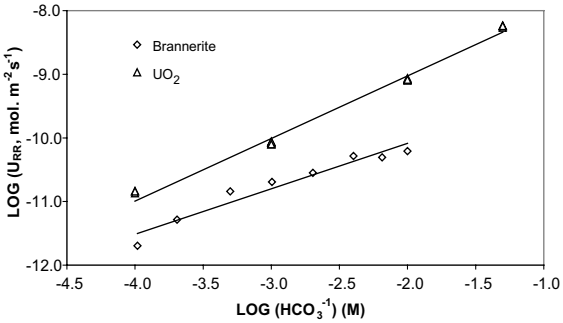


Fig. 7. The effect of bicarbonate (pH 8) on the uranium release rate from brannerite and $UO_2$ [15].

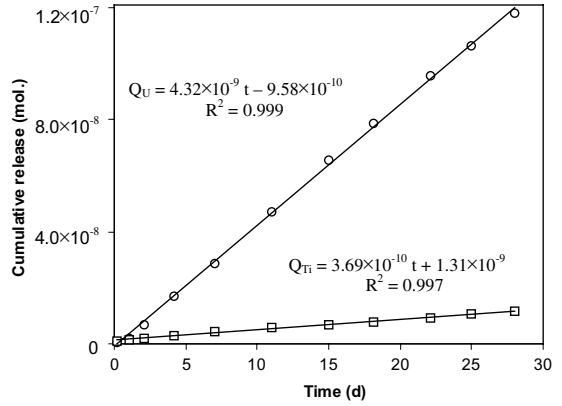


Fig. 8. Cumulative elemental releases versus time for dissolution of IBT specimen in pH 2 solution.

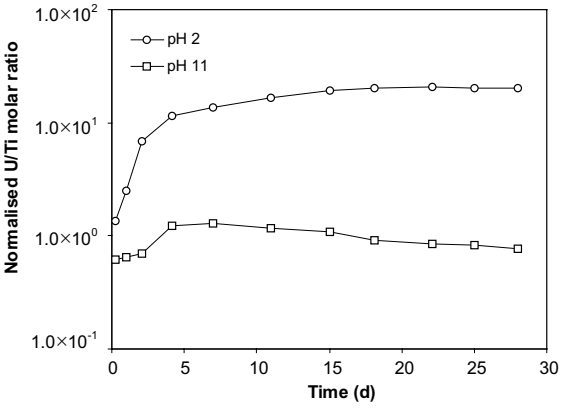


Fig. 9. Normalised U/Ti molar ratio in solution for the IBT specimens leached in different pH solutions.

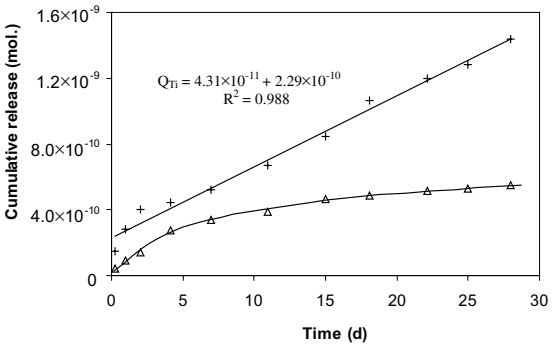


Fig. 10. Cumulative elemental releases versus time for dissolution of IBT specimen in pH 11 solution.

the Teflon vessel wall. Overall, the dissolution of the IBT specimen in pH 11 solution appears to be nearly congruent (Fig. 9).

### 3.4. TEM examination of IBT specimens

The IBT specimen exposed to pH 11 solution at 90 °C for 4 weeks shows large areas of a fibrous secondary phase associated with the original brannerite (Fig. 11(a)). In contrast, primary rutile ($TiO_2$) appears to be unaffected (not shown in Fig. 11). EDX spectroscopy shows that the Ti-rich secondary phase contains varying amounts of uranium and trace amounts of other elements, although the remaining underlying brannerite makes determination of the secondary phase composition difficult. Selected area electron diffraction indicates that the secondary phase is amorphous (Fig. 11(b), inset).

Compared to the pH 11 specimen, the IBT specimen leached in pH 2 solution at 90 °C for 4 weeks shows large areas of apparently unaltered brannerite as well as a relatively small amount of secondary phase. The primary rutile grains appear to have been partially etched (Fig. 12(a)). EDX spectroscopy indicates that the secondary phase is mainly $TiO_2$ with differing amounts of uranium and trace amounts of other elements. Selected area electron diffraction confirms that the secondary phase is polycrystalline, probably anatase and/or brookite (Fig. 12(b), inset).

### 3.5. XPS examination of IBT specimens

The two leached IBT specimens (in the pH 11 and pH 2 solutions respectively), as well as an unleached IBT specimen, were examined by XPS. C was the only impurity detected on the unleached specimen. The carbon signal was due to ubiquitous hydrocarbons present on all solid surfaces exposed to ambient air. The specimen leached in the pH 11 solution was found to contain U, Ti, O, C and a small amount of K and Ca on the surface. The source of K was from the leach solution (KOH) not having been rinsed off completely, while Ca was a minor contaminant in the leach solution (see above). The detection of Ca on the specimen surface (pH 11) is consistent with the results of TEM and solution analyses. The only impurities detected on the specimen surface leached in the pH 2 solution were C and a small amount of N; the presence of N was the result of $HNO_3$ solution not having been rinsed off completely.

The binding energy of the U $4f_{7/2}$ peak is directly related to the oxidation state of uranium. As the oxidation state of uranium increased from $U^{4+}$ ($UO_2$) to

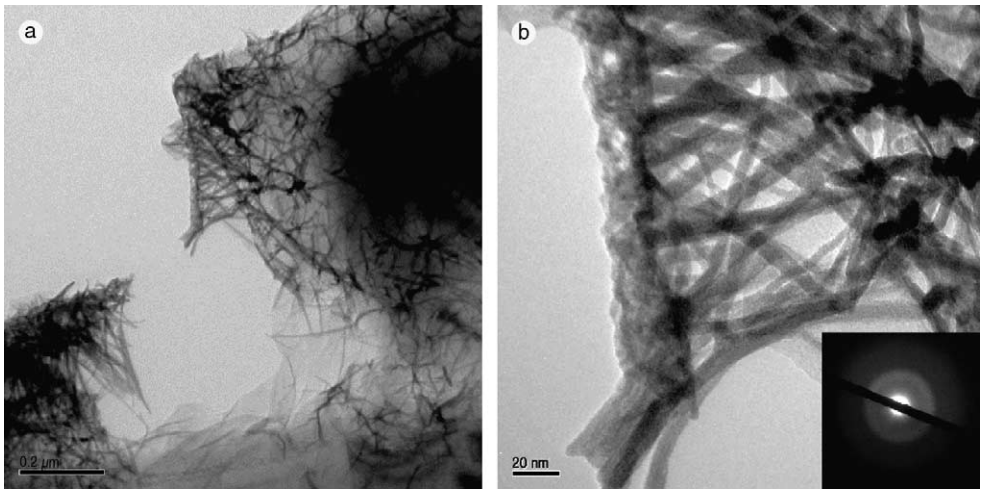


Fig. 11. TEM bright field image of IBT specimen dynamically leached in pH 11 solution at 90 °C for 4 weeks.

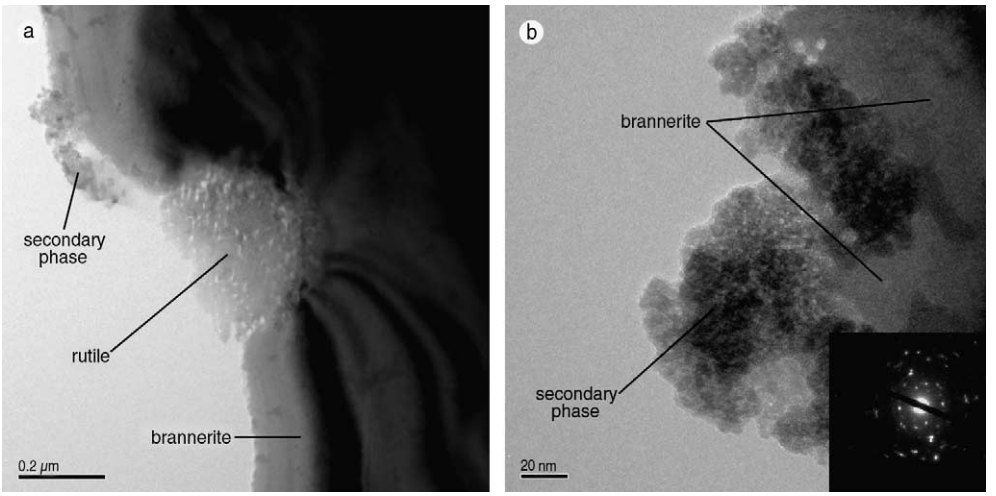


Fig. 12. TEM bright field image of IBT specimen dynamically leached in pH 2 solution at 90 °C for 4 weeks.

$U^{6+}$ ($UO_3$), the binding energy of the U $4f_{7/2}$ peak was observed to increase by 1.7 eV [16]. Fig. 13(a)–(c) show the U $4f_{7/2}$ XPS spectra of the brannerite surface prior to leach testing and after leaching in the pH 2 and 11 solutions, respectively. It is evident from the peak shape that there is more than one U species present on the surface of these samples. In order to separate the different components, each spectrum was fitted with three 50% Gaussian/50% Lorentzian curves after background subtraction. The peak position and width were allowed to vary freely, but the width of the three peaks was set to be equal in each fit (the spectra could not be fitted satisfactorily with fewer than three peaks). The peaks in each spectrum located at $(379.9 \pm 0.1)$ and $(380.9 \pm 0.1)$ eV were attributed to $U^{4+}$ and $U^{5+}$, respectively [14]. Compared with literature data, the binding energy of $U^{4+}$ formed here is similar to that of $U^{4+}$ in $UO_2$ [16]. The third peak, assigned as the $U^{6+}$ component, is located at $(382.0 \pm 0.1)$ eV for the unleached and pH 2 surfaces, but is found at 381.6 eV for the pH 11 specimen (similar to that of $U^{6+}$ in $UO_3$ [16]). When the $U^{6+}$ component is relatively small as a result of surface oxidation, its binding energy seems to shift to a value slightly higher than that for $U^{6+}$ in $UO_3$ [14].

As seen in Fig. 13(a), the brannerite surface prior to leach testing already contained a large amount of $U^{5+}$ probably as a result of surface oxidation due to the ion-beam-thinning procedure. The distribution of the $U^{4+}$, $U^{5+}$ and $U^{6+}$ components on the surface was quite similar to that leached in the pH 2 solution (Fig. 13(b)). The specimen leached in the pH 11 solution, however, was oxidised much more than the pH 2 specimen (Fig. 13(c)). This would support the conclusion that $U^{6+}$ was incorporated in the long fibrous U-bearing but Ti-rich alteration product covering a high percentage of the pH 11 specimen surface, as observed by TEM. The U/Ti

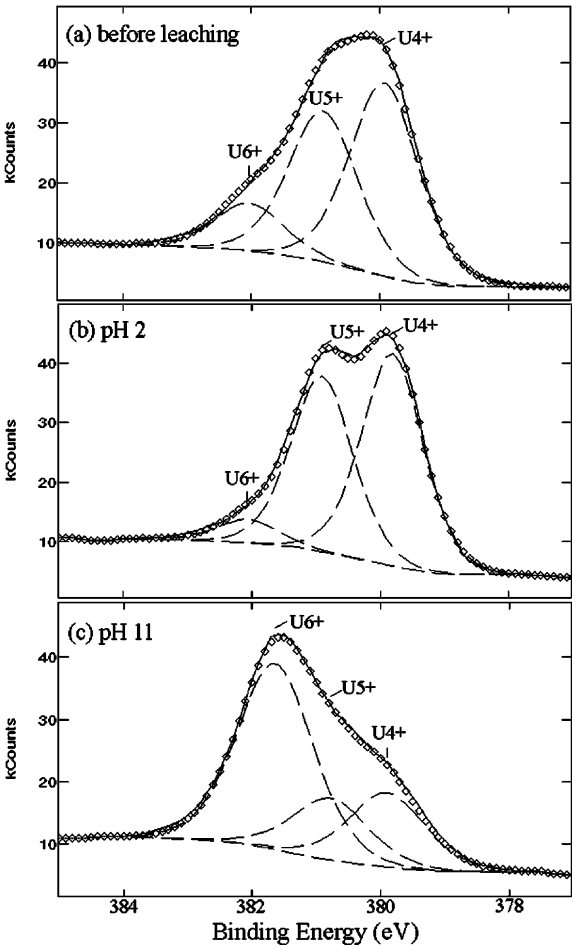


Fig. 13. U $4f_{7/2}$ XPS spectra of the brannerite surface (a) before leaching, and after leaching in the (b) pH 2 and (c) pH 11 solutions.

ratio determined from XPS was reduced from 0.59 before leaching to 0.37 after leaching in the pH 2 solution, consistent with the conclusion of preferential release of uranium at pH 2. Since large areas of the pH 11 surface were covered by an alteration product layer thicker than the probing depth of XPS ($\leqslant 5$ μm), the U/Ti ratio of the pH 11 surface (0.46) does not reflect the true U/Ti ratio of the leached brannerite surface. Note that since the sensitivity factors were not calibrated, the experimentally determined surface concentrations might deviate somewhat from the actual ones. But this systematic error is unimportant in the present context, as we are only comparing the surface composition of the three specimens.

### 3.6. Comparison with natural brannerite

The current and previous studies on the dissolution of synthetic brannerite in acidic solutions under atmospheric redox conditions revealed preferential release of uranium over titanium and polymorphous $TiO_2$ as the main alteration products, which are consistent with the observation for natural samples [17].

## 4. Conclusions

Although phthalate can increase the solubility of titanium, it has no significant effect on the dissolution of brannerite in a pH 4 buffer solution under atmospheric condition since the dissolution of uranium is dominant and generally over 100 times higher than that of Ti. Bicarbonate at pH of 8 increases the uranium release rate and therefore enhances the dissolution of brannerite. The dissolution of IBT specimens in under-saturated conditions in pH 2 ($HNO_3$) and pH 11 (KOH) solutions indicate: (1) higher elemental releases at pH 2 than those at pH 11; (2) preferential release of uranium at pH 2 and close to stoichiometric release at pH 11; (3) a polymorph at pH 2 and fibrous Ti-rich material at pH 11 as secondary phases. Overall, brannerite is more resistant to dissolution than $UO_2$ in both acidic and alkaline solutions, under atmospheric conditions.

## Acknowledgements

We thank M. Carter for fabricating synthetic brannerite and E.R. Vance for valuable comments on the manuscript.

## References

[1] B.B. Ebbinghaus, R.A. VanKonynenburg, F.J. Ryerson, E.R. Vance, M.W.A. Stewart, A. Jostsons, J.S. Allender, T. Rankin, J. Congdon, Ceramic Formulation for the Immobilization of Plutonium, Waste Management 98 (CD-ROM), Tucson, AZ, USA, 5 March, 1998.
[2] J.T. Szymanski, J.D. Scott, Can. Mineral. 20 (1982) 271.
[3] N. Waber, H.D. Schorscher, T. Peters, J. Geochem. Explor. 45 (1992) 53.
[4] R.O. Ifill, A.H. Clark, W.C. Cooper, CIM Bull. 82 (1989) 65.
[5] R.O. Ifill, W.C. Cooper, A.H. Clark, CIM Bull. 89 (1996) 93.
[6] G.R. Lumpkin, K.L. Smith, M.G. Blackford, R. Giere, C.T. Williams, Micron 25 (1994) 581.
[7] Y. Zhang, K. Hart, W. Bourcier, R.A. Day, M. Colella, B. Thomas, Z. Aly, A. Jostsons, J. Nucl. Mater. 289 (2001) 254.
[8] Y. Zhang, G.R. Lumpkin, B.S. Thomas, Z. Aly, R.A. Day, K.P. Hart, M. Carter, R. Cidu (Ed.), Water–Rock Interaction, 2001, p. 439.
[9] Y. Zhang, K.P. Hart, B. Thomas, Z. Aly, H. Li, M. Carter, in: K.P. Hart, G.R. Lumpkin (Eds.), Mater. Res. Soc. Symp. Proc. 663 (2001) 341.
[10] D.E. Grandstaff, in: Water–Rock Interaction, 1980, p. 72.
[11] A.E. Ringwood, S.E. Kesson, K.D. Reeve, D.M. Levins, E.J. Ramm, in: W. Lutze, R.C. Ewing (Eds.), Radioactive Waste Forms for the Future, North-Holland, Amsterdam, 1988, p. 233.
[12] G.R. Lumpkin, K.L. Smith, M.G. Blackford, R. Giere, C.T. Williams, Micron 6&25 (1994) 581.
[13] K.G. Knauss, T.J. Wolery, Geochim. Cosmochim. Acta 50 (1986) 2481.
[14] K.S. Finnie, Z. Zhang, E.R. Vance, M. Carter, J. Nucl. Mater. 317 (2003) 46.
[15] J. de Pablo, I. Casas, J. Giminez, M. Molera, M. Rovira, L. Duro, J. Bruno, Geochim. Cosmochim. Acta 63 (1999) 3097.
[16] D. Chadwick, Chem. Phys. Lett. 21 (1973) 291.
[17] G.R. Lumpkin, S.H.F. Leung, M. Colella, in: R.W. Smith, D.W. Shoesmith (Eds.), Mater. Res. Soc. Symp. Proc. 608 (2000) 359.